

INFORMATION TO USERS

The most advanced technology has been used to photograph and reproduce this manuscript from the microfilm master. UMI films the text directly from the original or copy submitted. Thus, some thesis and dissertation copies are in typewriter face, while others may be from any type of computer printer.

The quality of this reproduction is dependent upon the quality of the copy submitted. Broken or indistinct print, colored or poor quality illustrations and photographs, print bleedthrough, substandard margins, and improper alignment can adversely affect reproduction.

In the unlikely event that the author did not send UMI a complete manuscript and there are missing pages, these will be noted. Also, if unauthorized copyright material had to be removed, a note will indicate the deletion.

Oversize materials (e.g., maps, drawings, charts) are reproduced by sectioning the original, beginning at the upper left-hand corner and continuing from left to right in equal sections with small overlaps. Each original is also photographed in one exposure and is included in reduced form at the back of the book.

Photographs included in the original manuscript have been reproduced xerographically in this copy. Higher quality 6" x 9" black and white photographic prints are available for any photographs or illustrations appearing in this copy for an additional charge. Contact UMI directly to order.

U·M·I

University Microfilms International
A Bell & Howell Information Company
300 North Zeeb Road, Ann Arbor, MI 48106-1346 USA
313 761-4700 800 521-0600

PREVIEW

Order Number 9019560

Dissociative attachment in CH_3Cl , CH_2Cl_2 , CHCl_3 and CCl_4

Chu, Shi-Chung, Ph.D.

The University of Nebraska - Lincoln, 1989

U·M·I

300 N. Zeeb Rd.
Ann Arbor, MI 48106

PREVIEW

Dissociative Attachment in CH_3Cl , CH_2Cl_2 , $CHCl_3$ and CCl_4

by

Shi-Chung Chu

A DISSERTATION

Presented to the Faculty of

The Graduate College in the University of Nebraska

In Partial Fulfillment of Requirements

For the Degree of Doctor of Philosophy

Major: Physics and Astronomy

Under the Supervision of Professor Paul D. Burrow

Lincoln, Nebraska

December, 1989

Dissociative Attachment in
 CH_3Cl , CH_2Cl_2 , $CHCl_3$ and CCl_4

Shi-Chung Chu, Ph. D.

University of Nebraska, 1989

Advisor: Paul D. Burrow

This dissertation presents an electron beam study of the dissociative attachment process in the chloromethanes. A novel design of a high sensitivity ion counting system was incorporated in this work.

Each chloromethane displays two peaks in the dissociative attachment cross section below an electron energy of 1 eV, with the first peak consistently at zero energy and the second peak ranging from 0.27 to 0.80 eV. A systematic increase of the dissociative attachment cross sections is observed each time a Cl atom replaces an H atom. The ratio of the cross sections near zero electron energy between the highest and lowest attachers, namely CCl_4 and CH_3Cl respectively, is approximately six orders of magnitude, consistent with the earlier swarm measurements.

Also included in this dissertation is the application of the dissociative attachment process to study gas-surface vibrational energy exchange. In this work, cool gas was allowed to flow through a heated tube and then intercepted by the electron beam at right angles. N_2O was used in this study because its dissociative attachment cross section is very sensitive to temperature, permitting us to use it as a diagnostic tool for the measurement of vibrational temperature.

TITLE

Dissociative Attachment in CH_3Cl , CH_2Cl_2 , CHCl_3 and CCl_4

BY

Shi-Chung Chu

APPROVED

DATE

Paul D. Burrow

Dec. 14, 1989

Robert J. Hardy

Dec. 14, 1989

Eugene M. Rudd

Dec. 14, 1989

James A.R. Samson

Dec. 14, 1989

Marjorie Langell

Dec. 14, 1989

SUPERVISORY COMMITTEE

GRADUATE COLLEGE

UNIVERSITY OF NEBRASKA

Acknowledgement

I would like to express my gratitude to my advisor, Prof. Paul D. Burrow, for his guidance and encouragement through the years. I am also grateful for the complete freedom that I have enjoyed in my research work.

The machinists of the Physics Department have done a superior job in constructing many of the devices that I have used in the experiment. They were always helpful and friendly. My special thanks go to Don Fuehring and Loren Marks whom I have bugged the most. John Kelty and his staff provided continual support for our electronic devices. I also thank them.

Ying-Yuan Hsu has helped me in many respects in computer interfacing. Yang-Soo Chung helped me to install the SIMION program for the ion trajectory simulation. The authors of the SIMION program, Dahl and Delmore (EG&G), are also acknowledged.

I would like to thank my friends, Nien-Tsu Chow and Andrew Chang, for all the good times we had during the years of my graduate study.

My wife Shawn deserves my appreciation for her love, support and patience. I also appreciate all the joy my daughter Melody has brought to me.

Finally, the financial support from the National Science Foundation is greatly appreciated.

To my parents

PREVIEW

Contents

1	Introduction	1
2	Background	7
2.1	Classification of Resonances	9
2.1.1	Shape or Single-Particle Resonances	9
2.1.2	Core-Excited Resonances	11
2.2	Magnitudes of Dissociative Attachment Cross Sections . . .	13
2.3	Isotope Effect	17
2.4	Temperature Effect	19
2.5	Ion Pair Formation	24
2.6	Experimental Techniques	26
2.6.1	Electron Beam Method	28
2.6.2	Electron Swarm Technique	32
3	The Ion Counting System	34
3.1	Motivation	34
3.2	The Previous Apparatus	36
3.2.1	The Trochoidal Electron Monochromator	36

3.2.2	The Collision Region	39
3.2.3	The Analyzer Region	41
3.3	New Collision Region	42
3.3.1	Design Considerations	43
3.3.2	Construction	47
3.3.3	Typical Potentials for Ion Transport	50
3.4	The Ion Counting System	54
3.4.1	The Multi-Channel Plate (MCP)	54
3.4.2	MCP Protection Circuit	55
3.4.3	MCP Configuration	58
3.4.4	Counting Electronics	60
3.5	Computer Interfacing	62
3.5.1	DAS-8 Timer/Counter Board	63
3.5.2	DAC-02 Digital to Analog Converter	67
3.5.3	The BASIC Program	67
3.6	The Vacuum System	68
3.7	Background Signal	69
4	Performance and Precautions	71
4.1	Kinetic Energy Discrimination	72
4.2	Potential Penetration into the Collision Region	75
4.3	The B Field Dependence	77
4.4	Kinetic Energy Distributions	82
4.5	Total DA Cross Section Measurements	86

4.5.1	Pressure Dependence	87
4.5.2	Electron Beam Current Dependence	88
4.6	Signal Dependence on MCP Voltage and Ion Impact Energy	92
4.7	Precautions to Avoid Impurity Problems	95
5	Results	97
5.1	Motivation	97
5.2	Cross Section Measurement	100
5.2.1	Energy Calibration	104
5.3	Purity of the Gases	108
5.4	Results	108
5.4.1	CH_3Cl	109
5.4.2	Discussion of the 7.4 eV Peak	126
5.4.3	CH_3Cl With Impurities	127
5.5	CH_2Cl_2	129
5.6	$CHCl_3$	132
5.7	CCl_4	135
6	Applications of Dissociative Attachment	141
6.1	The Gas Thermometer	141
6.2	The Accommodation Coefficient	143
6.3	Standard Oven	145
6.3.1	Thermal Equilibrium	145
6.3.2	Temperature Measurement	146
6.3.3	Background Correction	147

6.4	Tube Oven	148
6.5	Monte Carlo Calculation	153
6.5.1	The Position of First Collision	155
6.5.2	The Displacement Along the Tube Axis	158
6.5.3	Transmission Probability	160
6.5.4	The Average Number of Wall Collisions	160
6.5.5	Correction for the Wall Collision Distribution	163
6.5.6	Gas-Gas Collisions	168
6.5.7	Collision Rate Along the Tube Axis	171
6.6	Results of Tube Oven Experiments	174
6.7	Improvements	181
6.7.1	Kinetic Energy Effect	182
6.7.2	Efficient Cooling of MCP	182
7	Conclusions	184
	Bibliography	186
	Appendix	
A	Calculation of the Potential Distribution in the Grid Region	193
B	Basic Program for Control of Experiment	204
C	Monte Carlo Calculations	212
D	Simulation of the Ion Trajectories by Using the SIMION Program	221
E	Dissociative Attachment in Vinyl and Allyl Chloride, Chlorobenzene and Benzyl Chloride	233

List of Figures

2.1	Schematic diagram of shape resonance	10
2.2	Schematic potential energy curves illustrating a typical dissociative attachment process	15
2.3	O^-/O_2 at three different temperatures	20
2.4	H^-/H_2 cross section curves at 300 and 1400 K	22
2.5	Internal-state dependence of threshold DA cross sections in H_2 and D_2	23
2.6	Hypothetic potential energy curves showing ion pair formation process	25
2.7	Ion pair formation process for Br_2 and Cl_2	27
3.1	(a) Schematic diagram of the previous apparatus and the relative potentials along the path of the electron beam . . .	37
3.2	Top view of the collision region and the lens system	45
3.3	Schematic diagram of the new collision region and lenses . .	48
3.4	Negative ion yield dependence on voltage of lens L1	52
3.5	O^-/N_2O as a function of the applied voltage to lens L2 and L3	53

3.6	Protection circuit with LED indicators	56
3.7	Amplifier and component that control the relay	57
3.8	MCP configuration.	59
3.9	Block diagram of the signal processing units	61
3.10	Flow chart of the BASIC program for control of experiment	64
3.11	Configuration of counters	66
4.1	O^-/CO_2 at different pusher voltages	74
4.2	FWHM of Cl^-/CCl_4 illustrates the electron energy resolution dependence on pusher voltage	76
4.3	The Cl^-/CH_2Cl_2 and O^-/CO_2 as a function of energy for several values of the current through the Helmholtz coils. .	79
4.4	The ratio of the peak values between Cl^-/CH_2Cl_2 and O^-/CO_2 as a function of B field.	80
4.5	The kinetic energy dependence of O^- anions from CO_2 . . .	84
4.6	The kinetic energy dependence of O^- anions from CO_2 and Cl^- from the chloromethanes	85
4.7	The yield of O^-/CO_2 at the 4.4 eV and 8.2 eV peaks as a function of source chamber pressure.	89
4.8	The yield of O^-/N_2O at 2.25 eV as a function of the electron beam current.	91
4.9	Signals of Cl^- and O^- as a function of ion impact energy and their ratio.	93
4.10	Signal dependence on the applied voltage across the MCP and the anode.	94

5.1	Derivative of transmitted current as a function of electron impact energy in the chloromethanes, $CHCl_2F$ and CCl_2F_2	98
5.2	The negative ion yield of Cl^- from CH_3Cl and CH_2Cl_2 versus electron energy	101
5.3	The negative ion yield of Cl^- from $CHCl_3$ and CCl_4 versus electron energy	102
5.4	Total negative ion yield of CH_3Cl and CH_2Cl_2 as a function of electron energy.	106
5.5	Total negative ion yield of $CHCl_3$ and CCl_4 as a function of electron energy.	107
5.6	Total anion yield of CH_3Cl	110
5.7	Total anion yield of CH_3Cl against electron energy over a larger energy range in which ion pair production process is observed.	111
5.8	Comparison of our result in CH_3Cl and the work of Petrović et al. (1989).	115
5.9	The Neutral and ionic curves of CH_3Cl along the coordinate of $C - Cl$ bond	120
5.10	Comparison of DA cross sections versus energy in HCl and CH_3Cl	125
5.11	Anion yield of CH_3Cl presented with the existence of impurity.	128
5.12	The electron energy dependence of the anion productions from CH_2Cl_2 below 20 eV	130

5.13	Total anion yield of $CHCl_3$ as a function of electron energy.	133
5.14	The anion curves of CCl_4 against electron energy.	136
5.15	The energy dependence of the anion yield from CCl_4 up to ~ 20 eV	137
5.16	Cross sections of the chloromethanes on a semi-log scale . .	139
6.1	Semi-log plot of the O^-/N_2O anion signal at various tem- peratures. Reproduced from Chantry (1969)	142
6.2	Total anion yield of O^-/N_2O versus electron energy at vari- ous temperatures.	149
6.3	Flow chart of the FORTRAN program for Monte Carlo cal- culation.	154
6.4	Schematic diagram shows the geometric relations.	157
6.5	Transmission probability of the effusing molecules for various tube ratios.	162
6.6	Average number of wall collisions of the effusing molecules as a function of tube ratio.	164
6.7	Distribution of the number of wall collisions of the effusing molecules for $l = 10$	165
6.8	Distribution of the number of wall collisions of the effusing molecules for $l = 20$	166
6.9	Distribution of the number of wall collisions of the effusing molecules for $l = 30$	167
6.10	Collision rate along the tube for $l = 10$	172
6.11	Collision rate along the tube for $l = 30$	173

6.12 O^-/N_2O versus electron energy at three different tube oven temperatures. Tube ratio $l = 20$	176
6.13 O^-/N_2O versus electron energy at three different tube oven temperatures. Tube ratio $l = 25$	177
6.14 O^-/N_2O versus electron energy at three different tube oven temperatures. Tube ratio $l = 36$	178
6.15 O^-/N_2O versus electron energy at three different tube oven temperatures. Tube ratio $l = 46$	179
6.16 O^-/N_2O versus electron energy at three different tube oven temperatures. Tube ratio $l = 60$	180

List of Tables

5.1	DA cross sections at low energy peaks of the chloromethanes.	105
5.2	Rate constants and corresponding attachment cross sections of CH_3Cl for thermal electrons as measured by the swarm methods.	113
5.3	Peak energies obtained from ETS and DA measurements. .	119
6.1	transmission probability of effusing molecules.	161
6.2	Average number of wall and gas collisions for various mean free path and tube ratios.	170

Chapter 1

Introduction

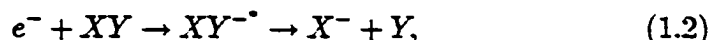
This dissertation deals with one particular type of electron-molecule interaction, namely the dissociative attachment (also referred to as DA hereafter) process. The first part of this work describes measurements of the DA cross section in a family of related molecules, i.e., the chloromethanes. Low energy electron impact on the chloromethanes has been studied experimentally by a number of authors (Scheunemann et al., 1980; Schultes et al., 1975 and references therein), but considerable disagreements about the magnitudes and shapes of the cross sections exist in the existing literature. To resolve these questions, more careful measurements in the chloromethanes are indispensable, which is the motivation of this work. The second part deals with the application of dissociative attachment in N_2O as a diagnostic tool in the study of the accommodation of vibrationally excited molecules on hot surfaces. The latter work was, in fact, carried out first and the requirement for improved detection sensitivity became the stimulus for the modified apparatus which is described in the first part of the work.

To give an outline of this dissertation, it begins with a general review of DA and the experimental methods to measure the DA cross sections in Chapter 2. Then in Chapter 3, the design and construction of the apparatus, i.e., the high sensitivity ion counting system, used in the present study to measure the cross sections of the chloromethanes are described. The performance of this ion counting system is evaluated in Chapter 4. Finally, in Chapter 5, the measured total DA cross sections of the chloromethanes are presented and discussed. An independent subject, the study of vibrationally excited N_2O on hot surfaces is discussed in Chapter 6. A little more detailed description of the contents in each chapter will be given later in this chapter.

Let us now examine the DA process which yields a neutral atomic or molecular fragment along with a stable negative ion upon electron impact as shown in Equation 1.1.



It can occur, therefore, only in molecules whose fragments have positive electron affinities. This process can be understood by first forming a temporary negative ion state



where e^- is the incident electron, XY is the target molecule and XY^{-*} is a temporary negative ion. Briefly, the incident electron is first captured by the target molecule to form a temporary negative ion, it then dissociates into an anion fragment and neutral fragment(s) if it survives the

autodetaching process. Thus, the magnitude of a DA cross section can be conveniently expressed as the capture cross section of the incident electron by the target molecule times a survival probability for dissociation.

In Chapter 2, these concepts are reviewed briefly along with the classifications of temporary anions. Shape and core-excited resonances, which play an important role in DA processes, are discussed. Temperature and isotope effects, which affect the magnitudes of DA cross sections, are also discussed. In addition to the DA process, ion pair formation, which proceeds without an intermediate temporary negative ion state, was also observed in the chloromethane molecules. Thus, a brief introduction regarding this process is also given. Finally, the experimental techniques used to study the DA process, primarily the electron beam and electron swarm methods, are described.

In Chapter 3, the high sensitivity ion counting system, designed for studying small signals is described. It begins with a discussion of the trochoidal electron monochromator which produces the monoenergetic electron beam. The electron beam is crossed by a molecular beam at right angles in the collision region. The collision region design is the result of several conflicting requirements, since we want to collect as many of the fragment ions as possible, which requires high draw-out voltages, and high energy resolution of the electron beam is still desired. The transport of negative ions from the collision region to the detector, a multi-channel plate (MCP) electron multiplier, is next discussed. Finally, the hardware and software that control the experiments are discussed.

The characteristics of the present ion counting system are described in Chapter 4. Knowledge of the system performance is important in determining the absolute total DA cross sections of the molecules under study. In particular, the role of discrimination against ions of different kinetic energies is examined by comparing with previously studied benchmark molecular systems such as CO_2 . The shielding properties of the present grid design in the collision region are studied along with the field dependence of the electron energy resolution. The linearity of the anion yield as a function of source chamber pressure and electron beam current are shown. The collection efficiency of the anion yield in the present counting system was found to be a function of the B-field and tests were carried out to determine the influence of this effect on our measurements.

The results of the total dissociative attachment cross section measurements in the chloromethanes are given in Chapter 5. Each molecule exhibits a sharp peak near zero electron energy and a relatively broad peak below 1 eV. The DA cross section increases rapidly when an H atom is replaced by a Cl atom, yielding a cross section ratio of more than 6 orders of magnitude between the zero energy peaks of CCl_4 and CH_3Cl .

The motivation for the high sensitivity apparatus was provided by a study in which we attempted to use the DA process as a diagnostic means to determine the vibrational temperature of a gas (N_2O) emerging from a tubular oven. Although this work was not brought to an entirely satisfactory conclusion, we have demonstrated that the concept is workable. A new study using the high sensitivity apparatus will be the subject for the

next generation of graduate student. The details of our preliminary work are discussed in Chapter 6. In short, the vibrational temperature of N_2O emerging from a tubular oven was found to be lower than the temperature of the oven, suggesting that vibrational thermal equilibrium condition has not been reached. With the high sensitivity apparatus, one expects to see the approach of the vibrational temperature of N_2O towards thermal equilibrium as N_2O molecules make *more* wall collisions within the tubular oven, in other words, as the length to diameter ratio of the oven is increased.

In Appendix A, a general equation used to calculate the potential around the collision region with grids that surround the electron beam is derived. A simplified model that simulates the design of the collision region is used in deriving this equation, hence the results are only approximate. Nevertheless, it gives us some insight about the potential distribution. The model used for deriving this equation incorporated equally spaced infinitely long line charges at equal distances which are parallel to the axis of an infinitely long cylindrical electrode. The line image charge method and superposition principle are used in the derivation. The variation of the potential for different numbers of line charges, the line charge location and different sizes of the line charge obtained by use of this equation are shown in Appendix A.

In Appendix B, a program written in the BASIC computer language which controls the counting experiment is listed. This program is written in such a way that the parameters such as the electron impact energy range, electron impact energy increment and the counting time interval for